

Research Article

Spectral Velocity of the Ground Surface in Alluvial Soils due to the Presence of Circular Urban Subway Tunnels

Hamed Fakhriyeh ¹, Reza Vahdani,² and Mohsen Gerami³

¹Assistant Professor of Civil Engineering, Islamic Azad University, Bojnourd Branch, Bojnourd, Iran

²Assistant Professor of Civil Engineering, Semnan University, Semnan, Iran

³Professor of Civil Engineering, Semnan University, Semnan, Iran

Correspondence should be addressed to Hamed Fakhriyeh; fakhrieh@bojnourdiau.ac.ir

Received 18 January 2022; Revised 22 February 2022; Accepted 4 April 2022; Published 25 April 2022

Academic Editor: Pengfei Wang

Copyright © 2022 Hamed Fakhriyeh et al. This is an open access article distributed under the Creative Commons Attribution License, which permits unrestricted use, distribution, and reproduction in any medium, provided the original work is properly cited.

In this study, the effect of urban subway tunnels with a circular cross section on the spectral velocity of the ground surface in alluvial soils was investigated. By changing the soil characteristics of the tunnel construction site and the geometric characteristics of the tunnel section (such as the radius and thickness of the lining and the depth of its placement), the frequency of the soil-tunnel system was changed. Then, the maximum velocity values were extracted for different parts of the ground surface. By averaging the data for each model, the amount of spectral velocity for different parts of the ground surface was extracted. The results show that the spectral velocity of the ground surface decreases by increasing the tunnel radius by 92% to a maximum of 12.3% in the tunnel center image on the ground's surface. Also, by increasing the doubling of the depth of the tunnel, the spectral velocity of the ground surface at a distance approximately equal to the radius of the tunnel is reduced to a maximum of 4.42%. The increase in the spectral velocity of the ground surface due to the increase in the depth of the tunnel is a maximum of 12.13% and occurs at a distance approximately equal to the tunnel radius. In a small number of reviewed models, increasing the depth of the tunnel placement increases the spectral velocity of the ground around the tunnel. The effect of increasing the thickness of the tunnel lining on the spectral velocity of the ground surface was also investigated. In tunnels with greater overhead depth, the spectral velocity of the ground surface increases by a maximum of 10.86% with increasing thickness of the tunnel lining and occurs in the image of the center of the tunnel on the ground surface. In tunnels with less overhead depth, the spectral velocity of the ground surface decreases by a maximum of 7.56% with increasing thickness of the tunnel lining and occurs approximately at a distance equal to the diameter of the tunnel from the image of the tunnel center to the ground surface. The study was performed using PLAXIS 2D and Ansys finite element software.

1. Introduction

Past studies have shown the importance of spectral velocity for buried structures such as urban subway tunnels. Because by increasing the thickness of the tunnel lining and strengthening the tunnel lining, the amount of energy absorbed by the tunnel structure increases and the energy is directly related to the second power of velocity. Therefore, many studies have been conducted to show the importance of spectral velocity, some of which are mentioned. Newmark et al. [1] used PGV to create an elastic spectrum. This trend was also considered for design regulations for structures in

the elastic spectrum in the Canadian Code [2]. In addition, PGV has been used in previous research to estimate the seismic damage of buried pipes [3, 4]. In previous research, experimental relationships for pipeline brittleness have been presented by Barenberg [5]; ALA [6]; Pineda and Ordaz [7]; and Jeon and O'Rourke [8] in terms of PGV. Past studies have also shown a correlation between PGV and the imported damage to structure, which can be referred to Hashash et al. [9, 10]. PGV is also used as an indicator of ground motion to determine the seismic behavior of a structure [11]. Akkar and Özen [12] investigated the effect of ground motion parameters on the inelastic requirements of

SDOF systems and reported the relationship between PGV and inelastic requirements for medium-period structures. PGV has also been used to estimate soil liquefaction [13]. [14] used PGV to evaluate the electricity network of Tehran. Correlations between PGV and assessed damages have also been observed in the studies by Porras and Najafi [15] and O'Rourke and Liu [16]. [17] showed that PGV can be considered as an indicator for estimating damage. Bastami and Soghrat [18] presented the velocity spectrum for the Iranian plateau. Studies also indicate the importance of spectral velocity in the near-field fault. Saito et al. [19] presented the velocity response spectra of the horizontal records at the lowest levels of the high-rise buildings in Miyagi, Tokyo, and Osaka cities. Also, "SV" is recommended for use in seismic design provisions for high-rise buildings [20].

Varnusfaderani et al. [21] studied the effects of initial seismic excitations near the fault and subsequent reverse fault rupture on cylindrical tunnels. They concluded that the pulse type determined by SVM_{ax} and PGV (indicating pulse intensity) and pulse period (TP) play a crucial role in the final response of the tunnel lining. Previous studies have not fully explained the effect of tunnels on ground surface velocity. Therefore, in this study, the effect of tunnel presence on "SV" was investigated.

2. Providing the Ground Surface Spectral Velocity due to the Presence of Tunnel

The present study investigates the effect of tunnels on the spectral velocity of the ground surface. Eleven world-famous earthquake records were applied to 36 models. About 500 nonlinear dynamic analyzes were performed. For the ground surface, points were taken at a distance of 0 and 5.83, 10.50, 15.17, 26.83, 38.5, and 51.33 meters from the image of the tunnel center. Different earthquake records were applied to the models and maximum velocities were taken for different points. In the next step, the tunnel characteristics, including the thickness of the tunnel lining and its diameter and depth of placement and alluvial soil characteristics are changed in order to change the frequency of the soil-tunnel system, and the above process is repeated. This process will result in the production of spectral velocity for the mentioned points, which will be averaged and average plus the standard deviation from the maximum velocities of the mentioned points. Ansys and PLAXIS 2D software were used for the study. Ansys was used for modal analysis and PLAXIS 2D for time history analysis.

2.1. Model Creation. The analysis of dynamic finite element of plain strain with rectangular range for models was performed. The dimensions of the models were considered 60×140 meters. A 15 nodal triangular element was considered for the soil and the tunnel lining was modelled with the plate element and elastically. Also, for modal analysis with Ansys, Drucker-Prager model was used for nonlinear soil properties and frequency-independent damping.

According to previous studies, the Mohr-Coulomb behavioural model was used in PLAXIS 2D [22, 24].

2.2. Properties of Main Model. In the present study, the Delhi subway was considered the main model. In the main model of the Delhi Metro tunnel, the radius is 3.13 meters, the overburden depth is 16.87 meters, the thickness of the tunnel lining is 0.28 meters, the modulus of elasticity is 3.16×10^7 kPa, and the Poisson's ratio (ν) is equal to 0.15.

Changes in the modulus of elasticity of alluvial soils with depth are summarized in Figure 1. Unit weight and saturation unit weight are equal to 18 and 20 kN/m³. The water table has been omitted. Soil cohesion (C) is equal to zero. The soil friction angle (ϕ) is 35° and the dilation angle (ψ) is 5°. The Poisson's (ν) is equal to 0.25. In order to consider the interaction between tunnel and soil in PLAXIS 2D, R_{inter} is used. According to the model specifications, R_{inter} in this study, was considered 0.67.

2.3. The Models Studied. A variety of models were reviewed in Table 1 for soil properties so as to make a wide range of frequencies for soil and tunnel set. These involve models with different elasticity modules for soil and different radius, lining thicknesses, and insertion depth for tunnel. Due to the fact that the soil in which the Delhi subway tunnel was created has a shear wave velocity less than 175 m/s, the modulus of soil elasticity was increased in such a way that the shear wave velocity did not exceed this value.

2.4. The Acceleration Records Used in the Study. The analyzes were performed by applying 11 different acceleration records to the models. The desired records were selected from PEER site. All the PGA acceleration records were scaled to 0.35 g using SeismoSignal software. It should be noted that PGA is considered "0.35 g" for the design of buildings in areas with a relatively high seismic risk, according to Iranian 2800 provisions. Chen et al. [26] studied the main frequency band of blast vibration signal based on wavelet packet transform. Their study showed that the main frequency band based on the computational method is a sensitive, accurate, and efficient frequency parameter; it can accurately describe the frequency characteristics of blasting signals and effectively overcome the drawbacks in Fourier transform.

Also, only the effect of earthquakes far fault has been studied. The effect of vertical earthquake components has been omitted in the study. Earthquakes were selected according to the soil characteristics of the models (soil shear wave velocity is less than 175 m/s for all models considered). Acceleration records and their spectra before and after scaling are shown in Figure 2.

2.5. Damping. PLAXIS 2D is a finite element software. In the finite element method, Riley damping is one of the suitable measurements that tolerates the damping effects in stiffness and mass matrices. Riley damping in plain strain models such as two-dimensional tunnels with earthquake

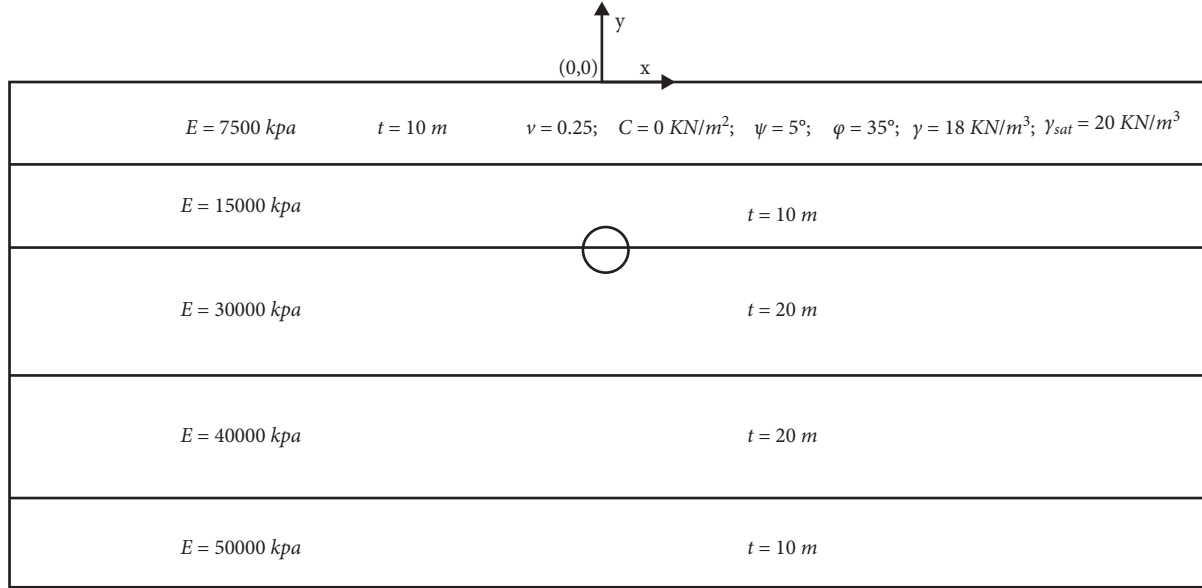


FIGURE 1: The properties of Delhi subway soil (main model) in different depths [25].

TABLE 1: Models considered in research.

No.	Elasticity module of soil (relative to the main model)	The depth of the tunnel (m)	Tunnel lining thickness (m)	Tunnel radius (m)	No.	Elasticity module of soil (relative to the main model)	The depth of the tunnel (m)	Tunnel lining thickness (m)	Tunnel radius (m)
1	1	20	0.5	3.13	19	1.75	20	0.5	6
2	1	20	0.28	3.13	20	2	20	0.5	3.13
3	1	10	0.5	6	21	2	20	0.28	3.13
4	1	10	0.75	6	22	2	10	0.75	6
5	1	20	0.75	6	23	2	10	0.5	6
6	1.25	10	0.28	3.13	24	2	20	0.5	6
7	1.25	20	0.28	3.13	25	2	20	0.75	6
8	1.25	10	0.5	6	26	2.25	10	0.28	3.13
9	1.25	20	0.5	6	27	2.25	20	0.28	3.13
10	1.5	20	0.5	3.13	28	2.25	10	0.5	6
11	1.5	20	0.28	3.13	29	2.25	20	0.5	6
12	1.5	10	0.75	6	30	2.5	20	0.5	3.13
13	1.5	10	0.5	6	31	2.5	20	0.28	3.13
14	1.5	20	0.5	6	32	2.5	20	0.5	6
15	1.5	20	0.75	6	33	2.5	10	0.5	6
16	1.75	10	0.28	3.13	34	2.5	10	0.28	3.13
17	1.75	20	0.28	3.13	35	1	20	0.5	6
18	1.75	10	0.5	6	36	1	10	0.28	3.13

application will have good results. The general form of Riley damping is in the form of equation

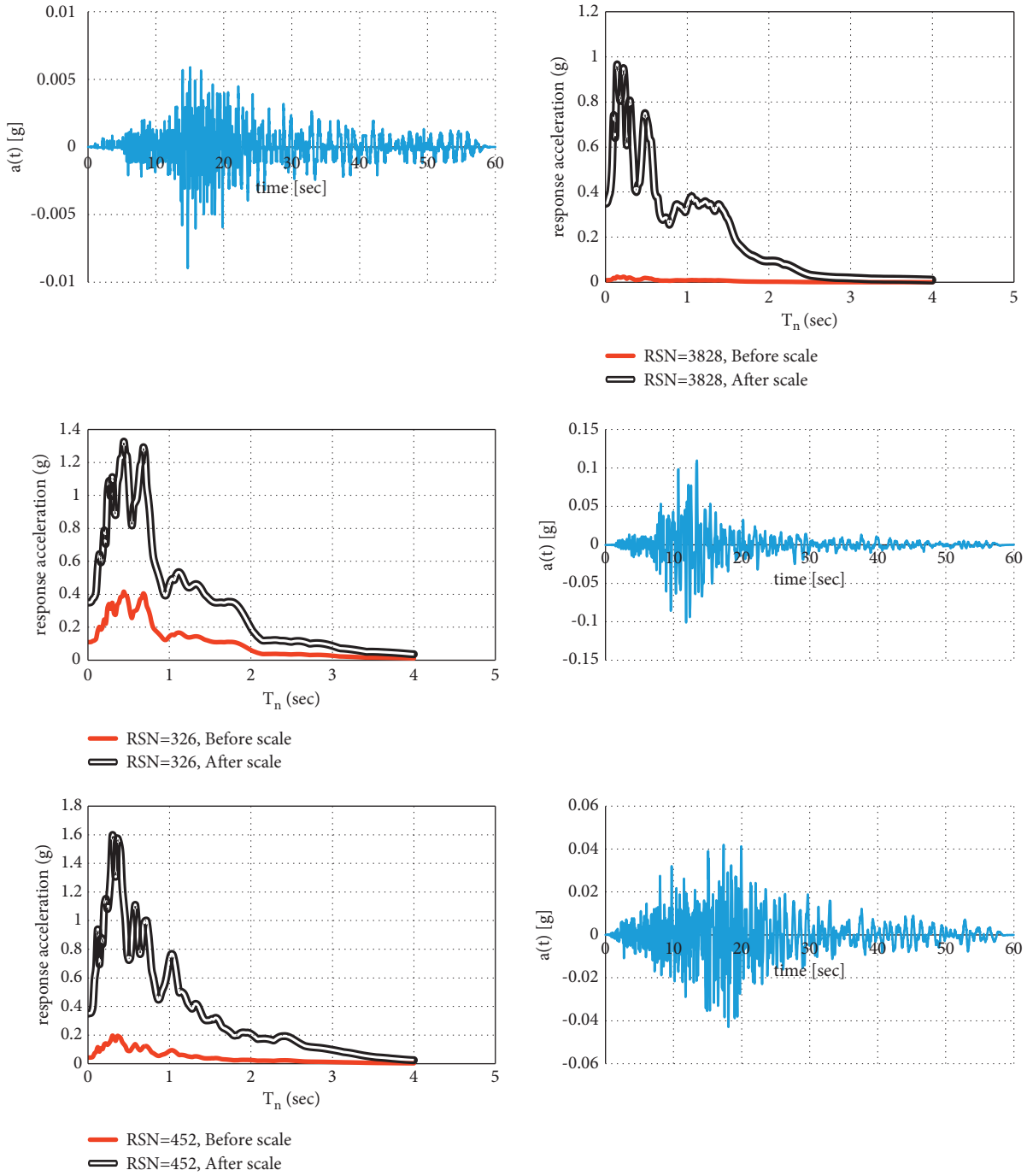
$$[C] = \alpha[M] + \beta[k]. \quad (1)$$

In this equation, K and M are the stiffness and mass matrices, and α and β are Riley damping coefficients, respectively. Riley alpha determines the mass effect and Riley beta determines the effect of stiffness on system damping. These coefficients are determined by equation (2).

$$\begin{Bmatrix} \alpha \\ \beta \end{Bmatrix} = \frac{2\xi}{\omega_n + \omega_m} \begin{Bmatrix} \omega_n \cdot \omega_m \\ 1 \end{Bmatrix}. \quad (2)$$

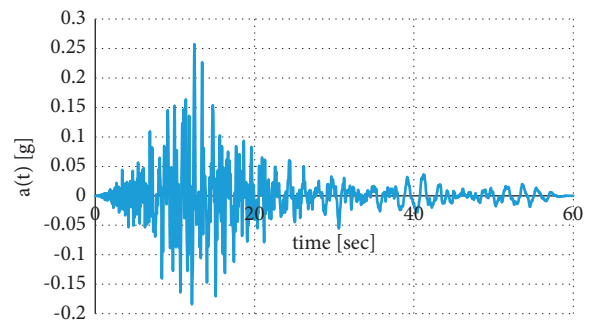
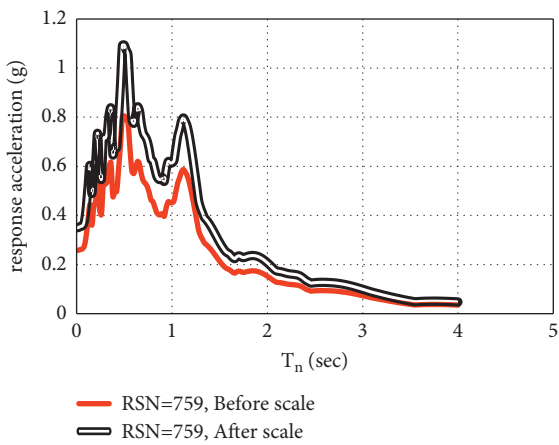
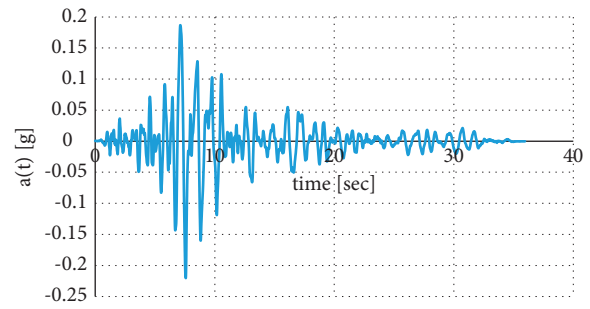
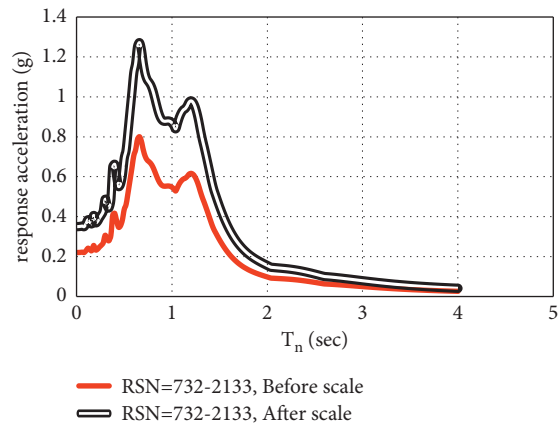
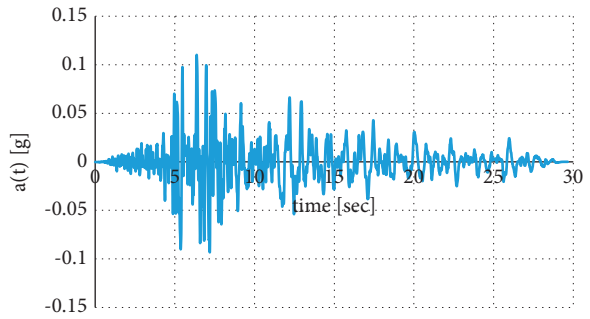
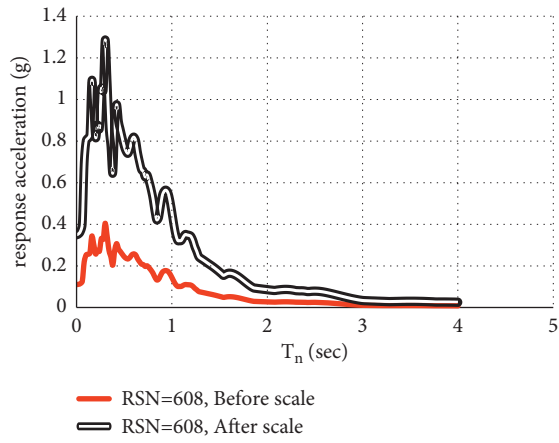
In this equation, ξ is the damping ratio and ω_n and ω_m are the natural angular frequencies in rad/sec for n and m modes. In this study, m and n were considered 1 and 2, respectively. The frequency of different modes was calculated with Ansys software for all models in Table 1. Riley's alpha and beta were then calculated with a 5% damping assumption and used to analyze time history in PLAXIS 2D.

2.6. Boundary Conditions. The boundaries were considered far enough away to prevent refraction and reflection of the wave. According to previous research, to achieve free field conditions, the distance between the tunnel and the lateral

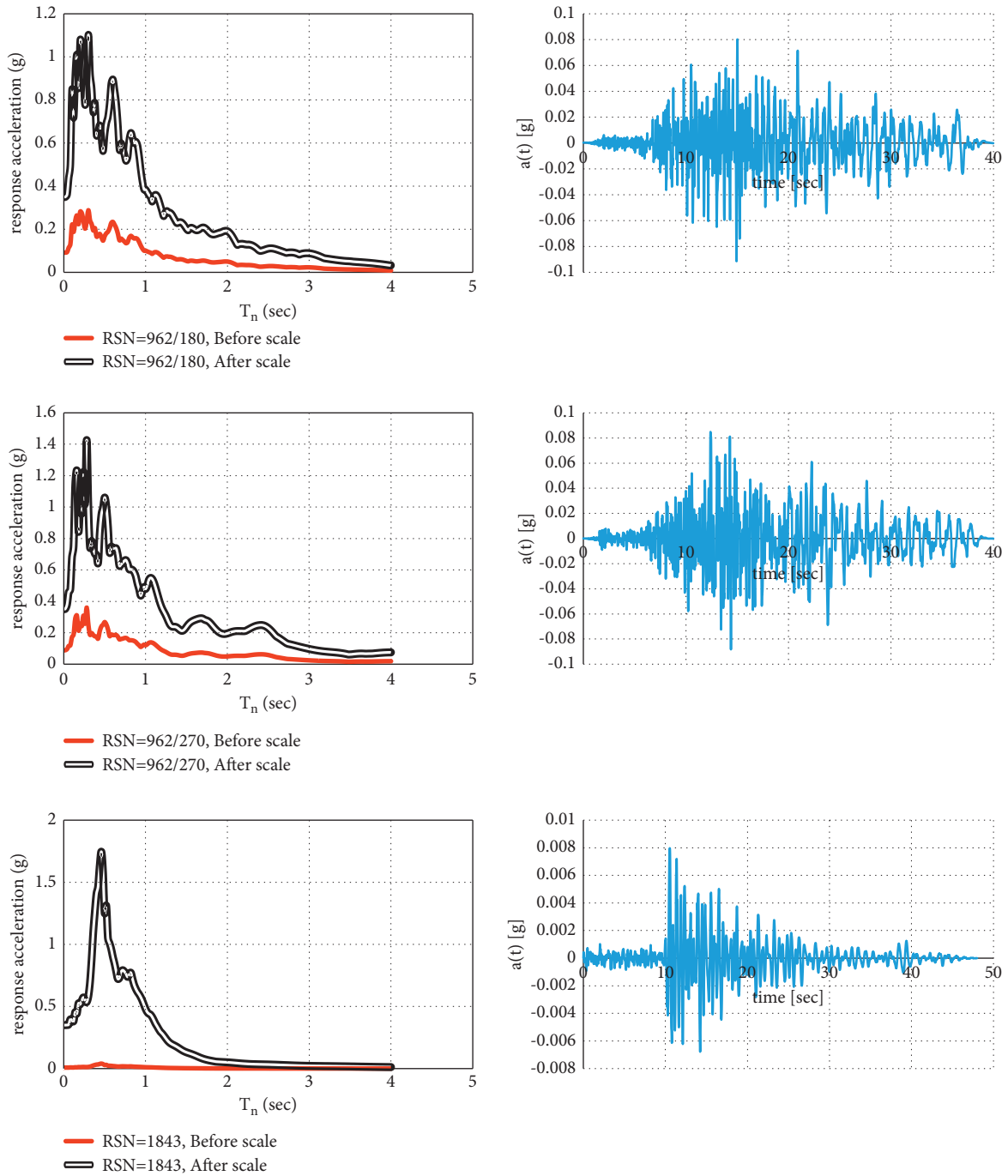


(a)

FIGURE 2: Continued.



(b)
FIGURE 2: Continued.



(c)
FIGURE 2: Continued.

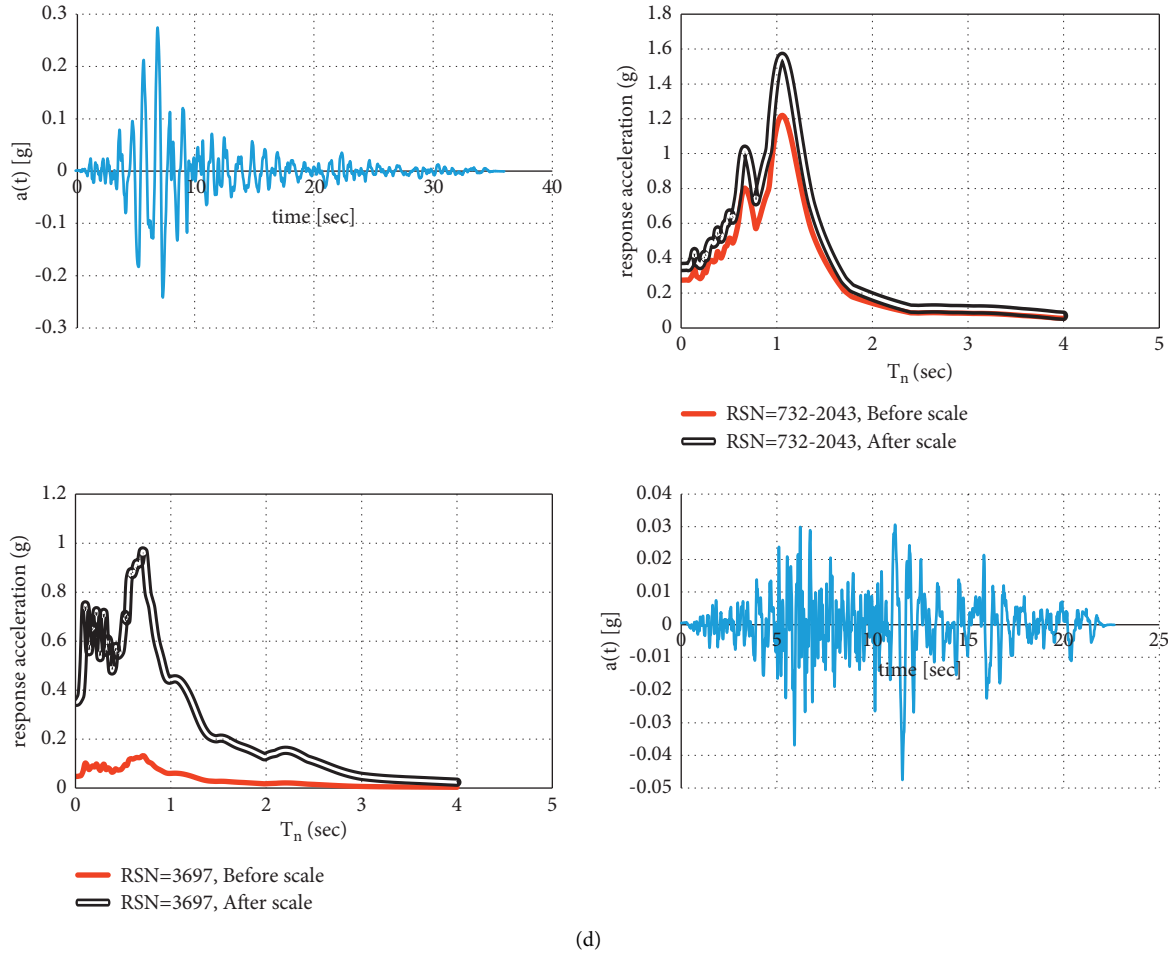


FIGURE 2: Acceleration records used in the study and comparison of their response spectrum before and after scaling PGA to 0.35 g.

boundaries of the model was considered 5 times the diameter of the tunnel (5D) [22]. Due to the fact that two types of static and dynamic analyses were considered, so for static analysis, the nodes were bounded along the vertical boundaries of the finite element mesh in the x direction and are free in the y direction and at the bottom boundaries in both x and y were bounded. Viscous absorbent boundaries were used for dynamic analysis proposed by [27]. Viscose boundaries include a dashpot which are corresponding to each degree of freedom at each node along the boundaries.

2.7. Analysis Phases. Modal analysis was performed using Ansys. Using modal analysis, the frequencies of the soil-tunnel system were obtained for all the models in Table 1. Using the first and second mode frequencies for all models in Table 1, Riley alpha and beta were calculated. The following three phases were considered for analysing the time history in PLAXIS 2D:

- (i) In phase one, plastic calculation and stage construction were performed. At this stage, tunnel lining became active and its internal soil got inactive.

- (ii) Second phase consists of soil excavating simulation through contraction of tunnel lining. Contraction was accounted 2% for the center of the tunnel.
- (iii) Third phase contains the nonlinear time histories analysis and employment of the acceleration records once the plastic calculations are performed.

In PLAXIS 2D, the implicit Newmark design is used for numerical time integral calculations. In the Newmark method, the optimal values of the selected parameters can be $\beta = 0.3025$ and $\gamma = 0.6$, which was used in PLAXIS 2D.

2.8. Verification. In the present study, two types of modal analysis and time history were performed. Modal analysis validation was performed with Sevim paper. Figure 3 shows the validation of the modal analysis with the [28] paper for the Arhavi Tunnel in Turkey for the second vibrating mode. As can be seen, the results are well matched. Validation results for time history analysis are shown in Figure 4. Validation of time history analysis was performed with Singh et al.'s (2016) paper for Delhi Metro tunnel. As can be seen from Figures 3 and 4, the results of the validation are in good agreement with the mentioned articles.

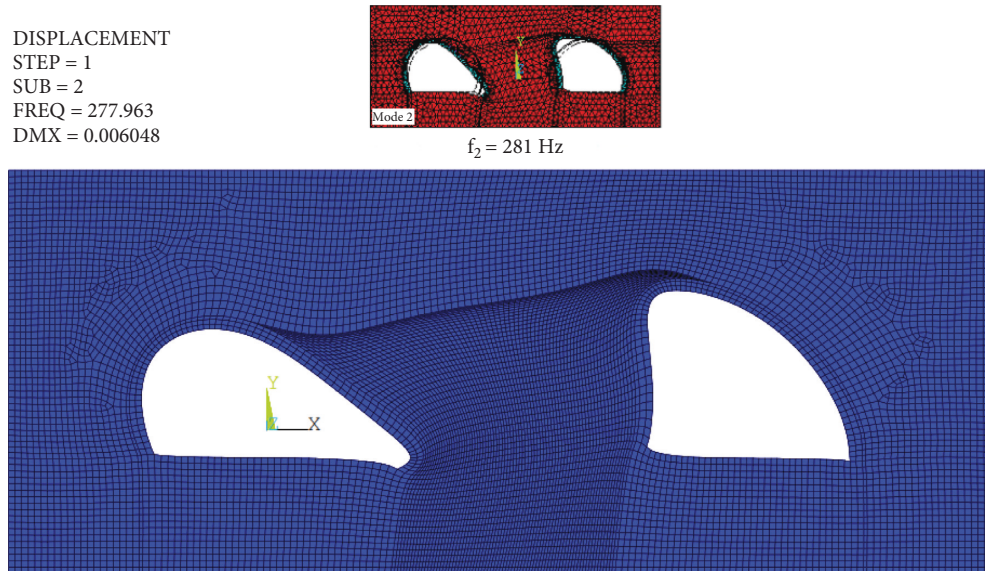


FIGURE 3: Comparison of validation modal analysis with Sevim (2011) article for the second vibrational mode of the Arhavi Tunnel in Turkey.

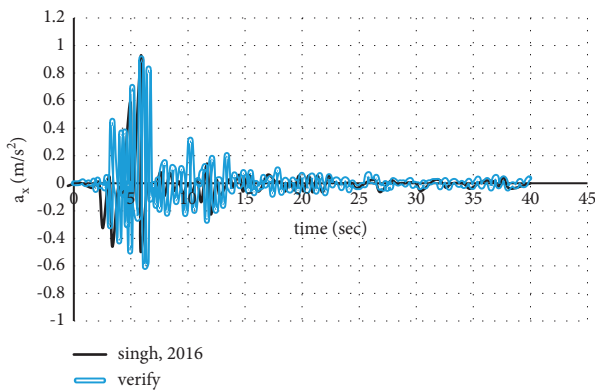


FIGURE 4: Comparison of validation time history analysis with Singh et al.'s paper for Delhi Metro tunnel to accelerate the point corresponding to the image of the center of the tunnel to the ground surface.

3. Time History Analysis and Review of Results

3.1. Parametric Study. According to the analysis, it was determined that with increasing the soil cohesion, the amount of maximum velocity decreases. Due to the fact that soil cohesion is considered zero ($C=0$) in the calculations, so the results of the study have a good reliability coefficient compared to other values of the soil cohesion. The effect of internal soil friction angle (f) on the results of the analysis was also investigated. This parameter was considered 35° in the analysis. It was investigated that the results of the study are in the range of friction angle of 20 to 40° with good accuracy, and outside this range, the results are less accurate. Also, the dilation angle (ψ) considered in the 5° analysis will have a small effect on the value of the considered maximum velocity of the points and reducing it will cause a very small increase in the spectral velocity. The effect of changes in soil unit weight on maximum velocity was also investigated. In

the analysis, unit weight and saturation unit weight are considered to be 18 and 20 kN/m^3 , respectively. With a decrease in unit weight to 14 kN/m^3 , changes of less than 3.5% in maximum velocity were observed. In the next step, the effect of Poisson's coefficient (ν) on the maximum velocity was investigated. It was found that changes in the Poisson's soil Poisson ratio would have a small effect on the maximum velocity.

Of all the soil parameters whose effect on the maximum velocity corresponding to the center of the tunnel to the ground surface has been investigated, the internal soil friction angle is the most important factor among all soil parameters in changing the maximum ground surface velocity.

3.2. Review of the Results of Time Histories Analysis. Modeling was performed in PLAXIS 2D to analyze the time history. The mean spectral velocity ($Sv\mu$) was calculated by averaging the maximum velocity values. The effect of changing the tunnel radius from 3.13 m to 6 m was investigated for points located on the ground. These points were selected at a distance of zero, 5.83 , 10.50 , 15.17 , 26.83 , 38.5 , and 51.33 meters from the image of the center of the tunnel on the ground surface. The results are shown in Figures 5 and 6.

As it can be seen from the above figures, in general, a tunnel with a smaller radius will cause a higher spectral velocity ($Sv\mu$) than a tunnel with a larger radius. However, with the distance from the image of the center of the tunnel on the ground surface, the difference between the values of spectral velocity for tunnels with different diameters will be less. Also, the spectral velocity ($Sv\mu$) for a smaller diameter tunnel is generally reduced by moving away from the image of the center of the tunnel on the ground surface. The opposite is hold true for larger diameter tunnels.

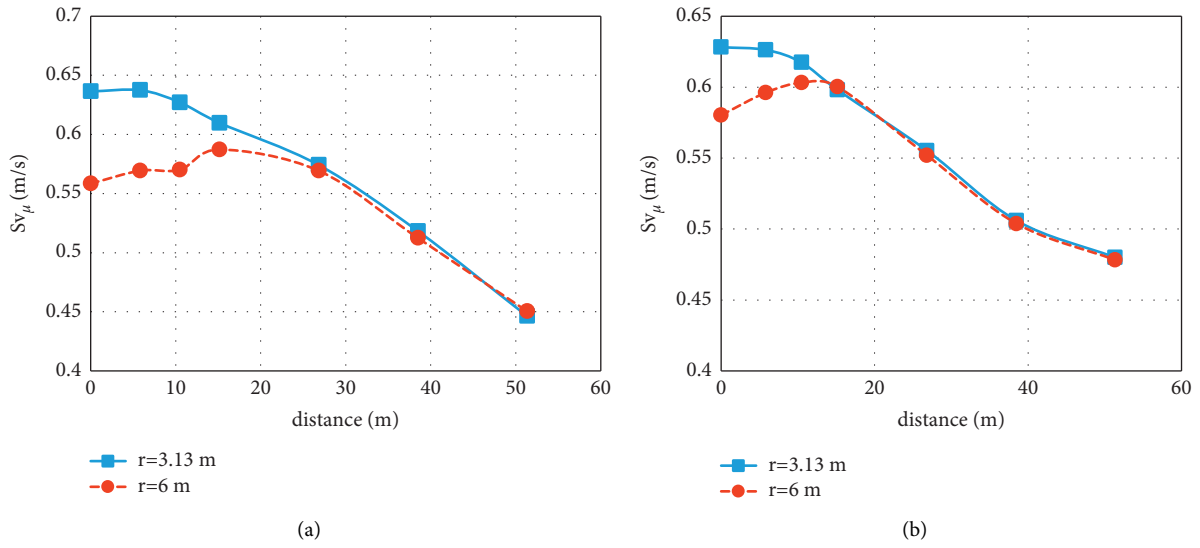


FIGURE 5: Effect of tunnel radius on ground surface velocity for models (a) 1 and 35 and (b) 10 and 14 of Table 1.

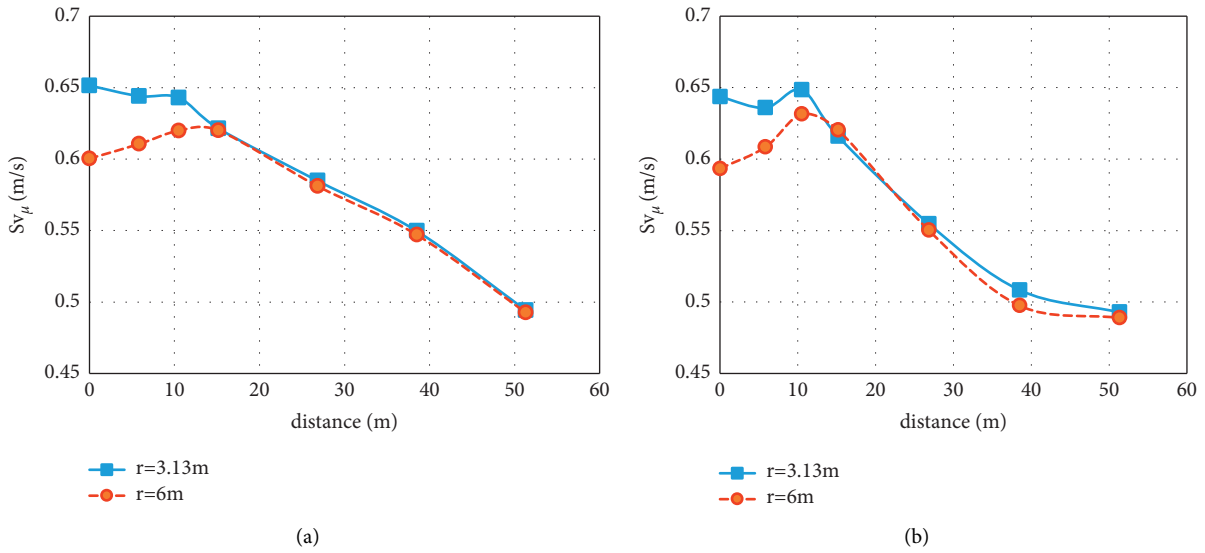


FIGURE 6: Effect of tunnel radius on ground surface velocity for models (a) 20 and 24 and (b) 30 and 32 of Table 1.

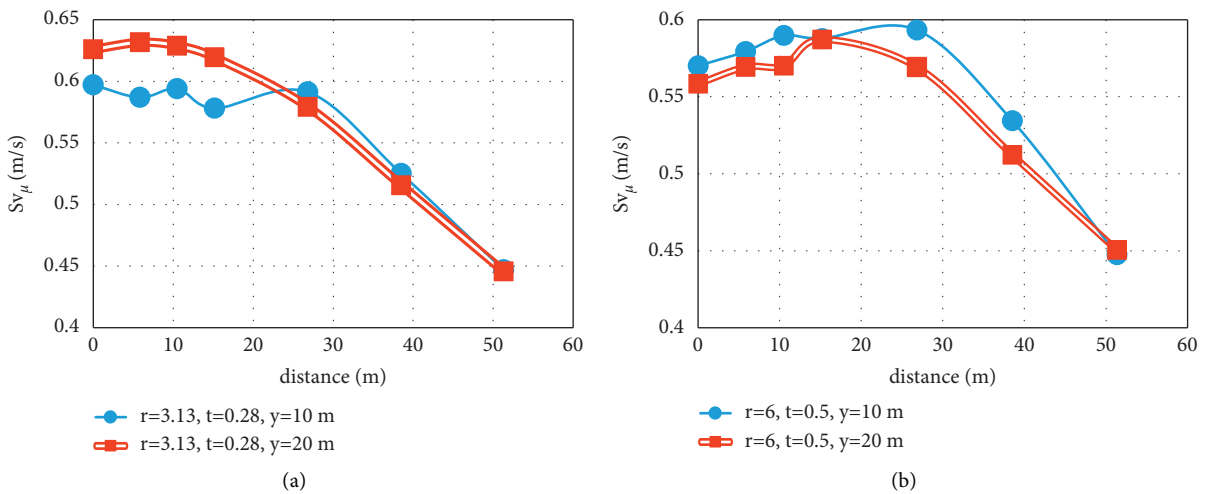


FIGURE 7: The effect of change in overburden depth on ground surface velocity for models (a) 2 and 36 and (b) 3 and 35 of Table 1.

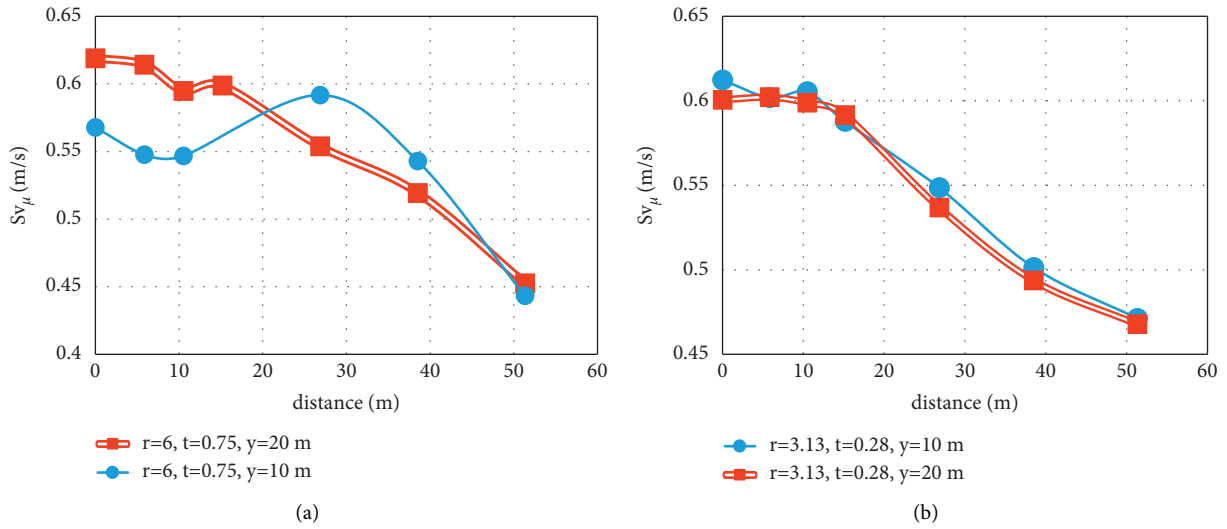


FIGURE 8: The effect of change in overburden depth on ground surface velocity for models (a) 4 and 5 and (b) 6 and 7 of Table 1.

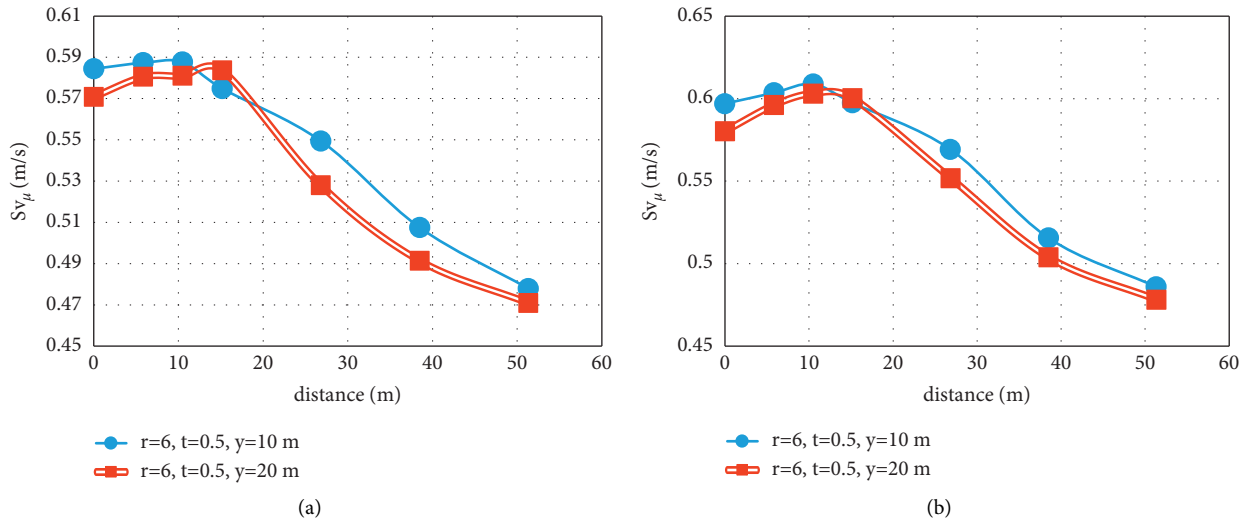


FIGURE 9: The effect of change in overburden depth on ground surface velocity for models (a) 8 and 9 and (b) 13 and 14 of Table 1.

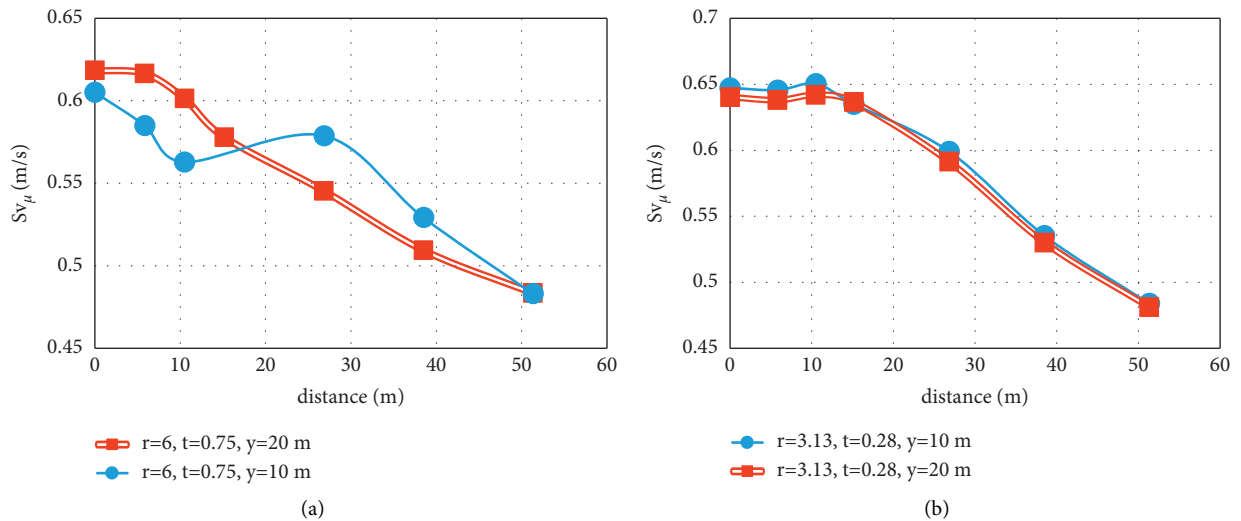


FIGURE 10: The effect of change in overburden depth on ground surface velocity for models (a) 12 and 15 and (b) 16 and 17 of Table 1.

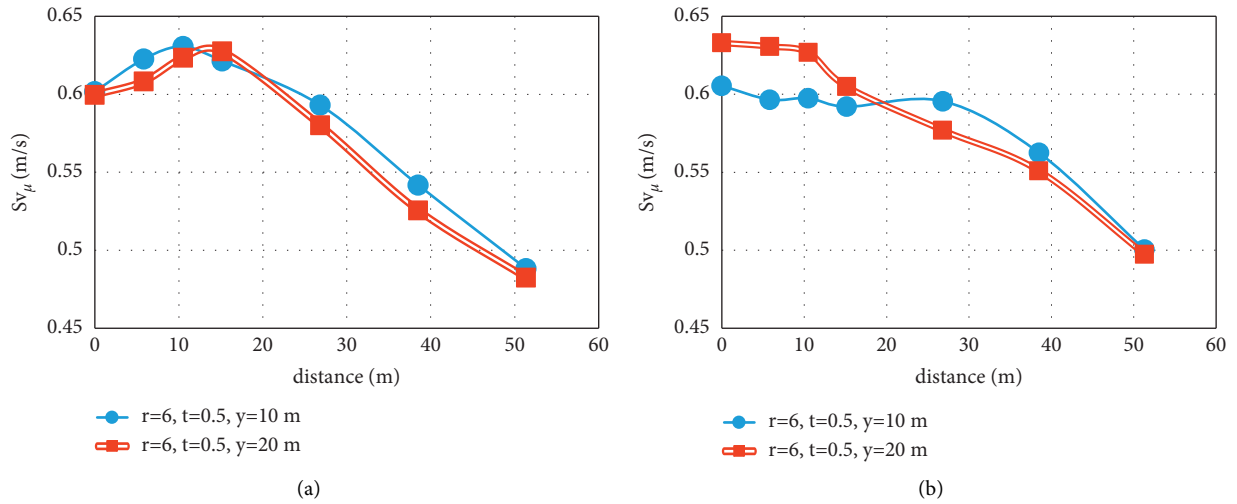


FIGURE 11: The effect of change in overburden depth on ground surface velocity for models (a) 18 and 19 and (b) 22 and 25 of Table 1.

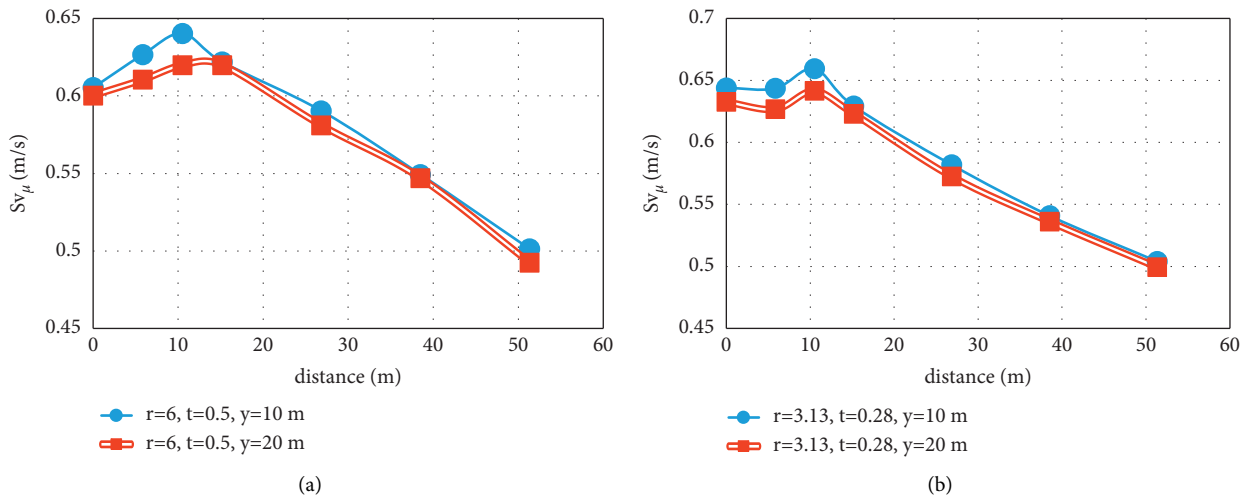


FIGURE 12: The effect of change in overburden depth on ground surface velocity for models (a) 23 and 24 and (b) 26 and 27 of Table 1.

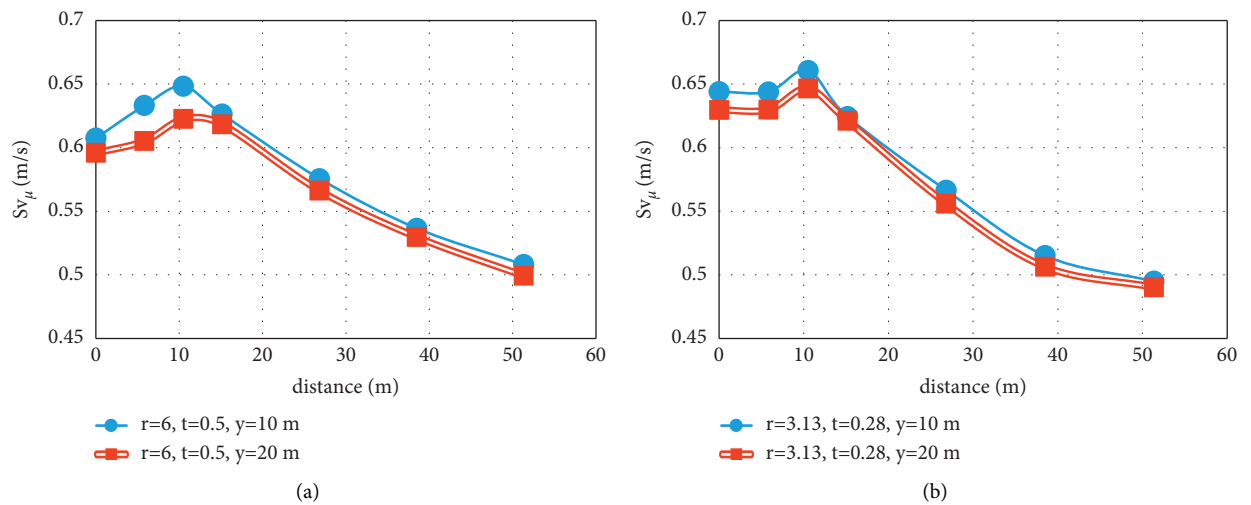


FIGURE 13: The effect of change in overburden depth on ground surface velocity for models (a) 28 and 29 and (b) 31 and 34 of Table 1.

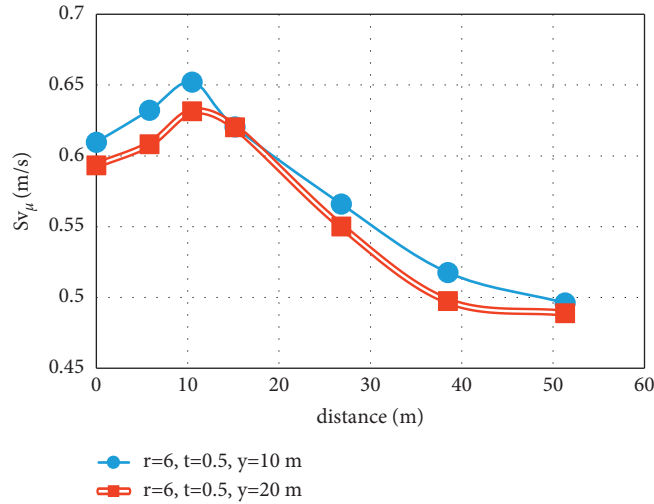


FIGURE 14: The effect of change in overburden depth on ground surface velocity for models 32 and 33 of Table 1.

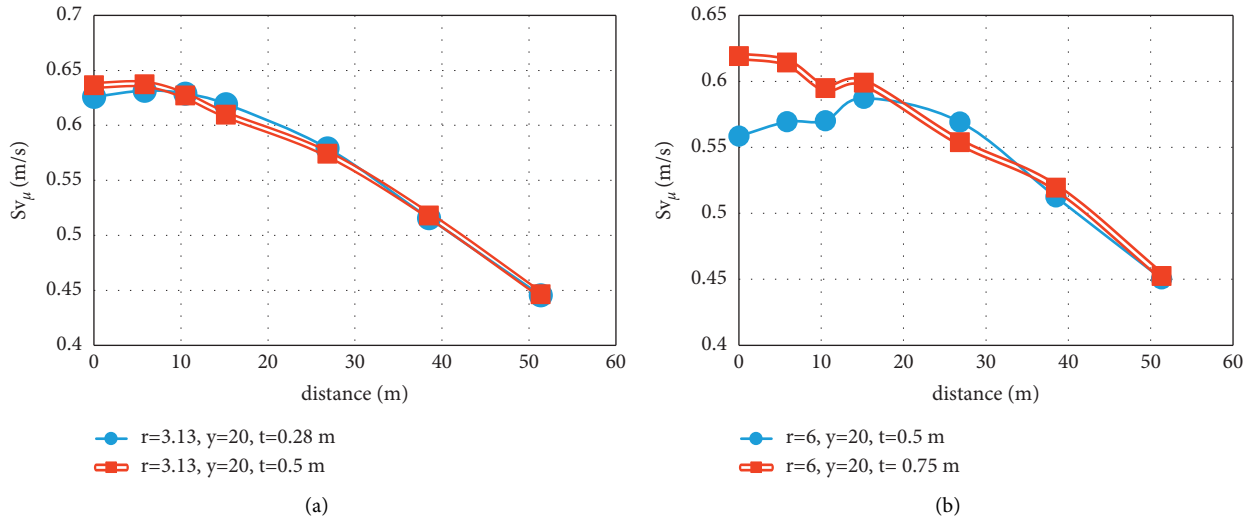


FIGURE 15: The effect of change in tunnel lining thickness on ground surface velocity for models (a) 1 and 2 and (b) 5 and 35 of Table 1.

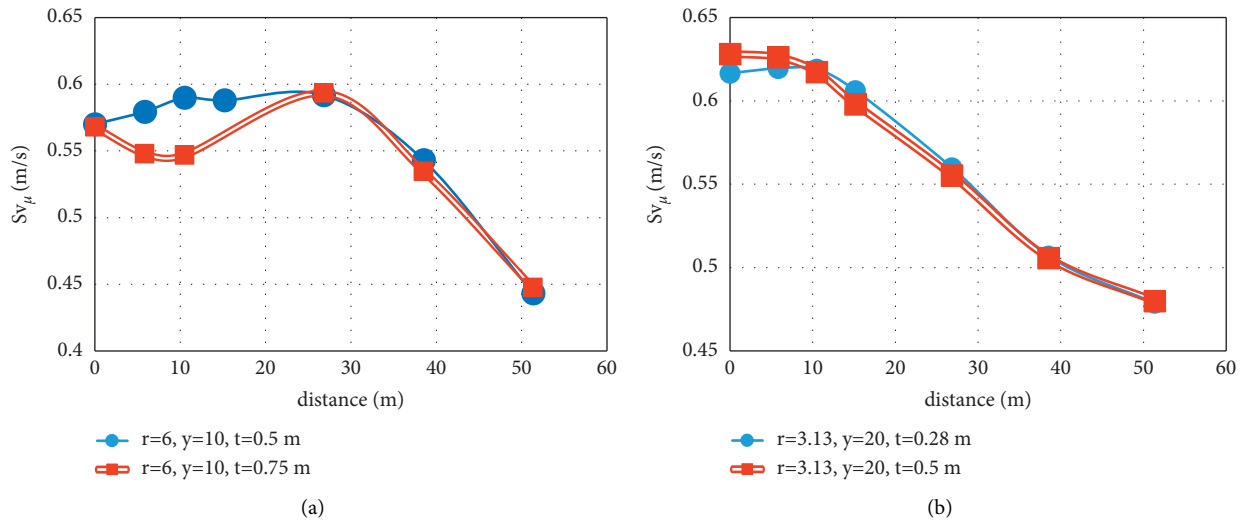


FIGURE 16: The effect of change in tunnel lining thickness on ground surface velocity for models (a) 3 and 4 and (b) 10 and 11 of Table 1.

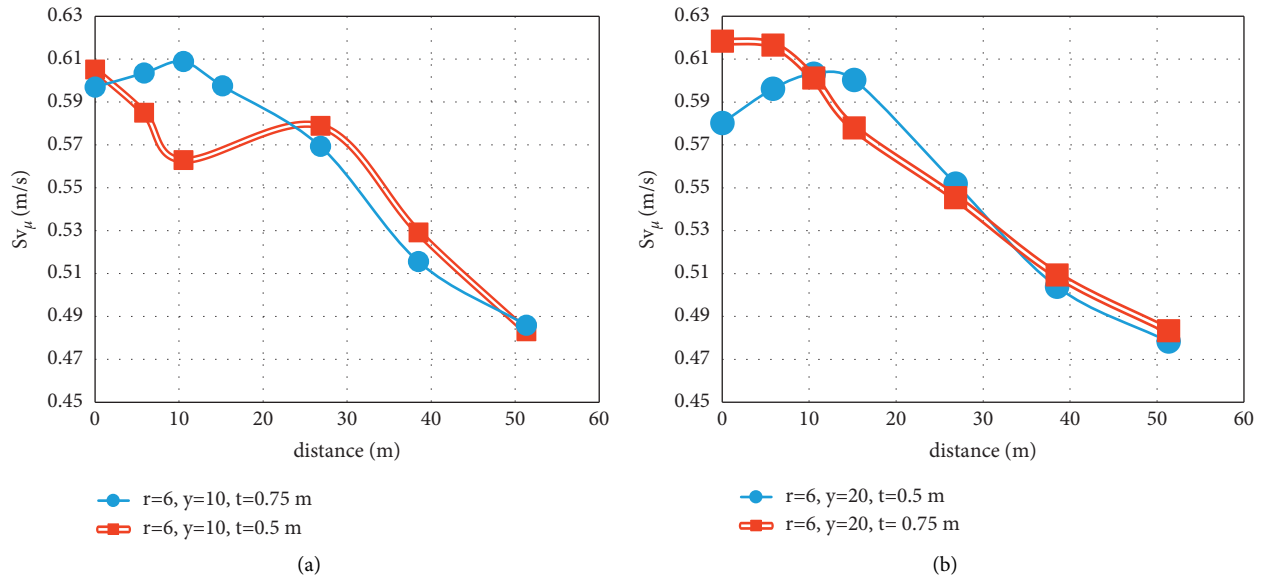


FIGURE 17: The effect of change in tunnel lining thickness on ground surface velocity for models (a) 12 and 13 and (b) 14 and 15 of Table 1.

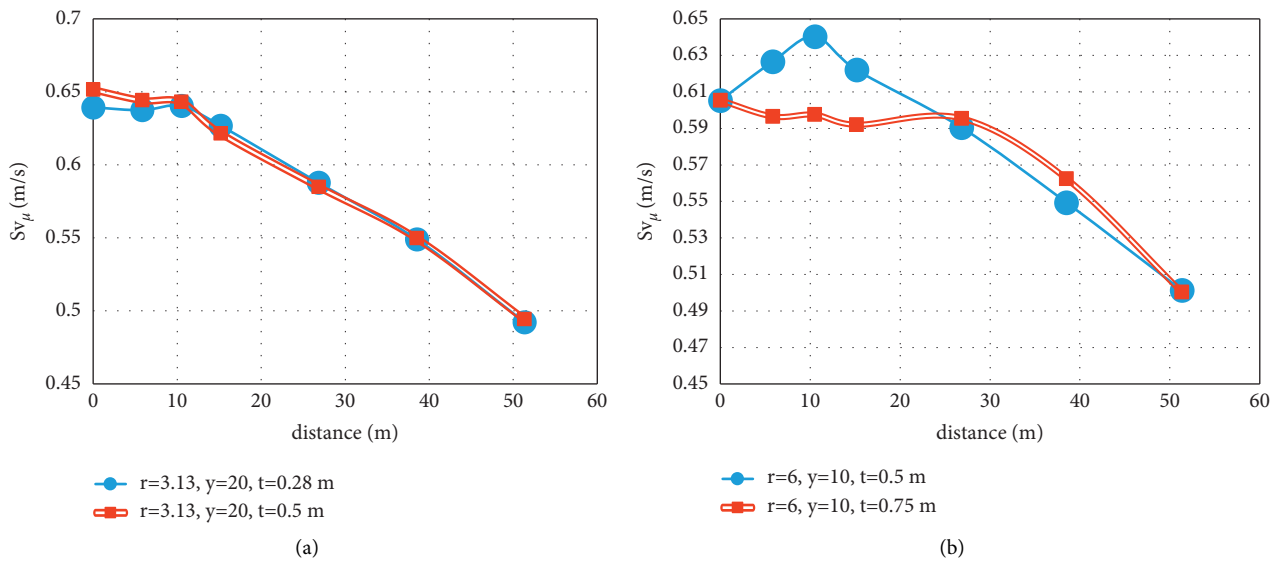


FIGURE 18: The effect of change in tunnel lining thickness on ground surface velocity for models (a) 20 and 21 and (b) 22 and 23 of Table 1.

By increasing the tunnel radius almost twice, the decrease in the spectral velocity of the ground surface occurs in the range of 0.84% to 12.3% depending on the distance of the point under study from the tunnel. The greatest decrease in the spectral velocity of the ground surface occurs due to the increase of the tunnel radius exactly in the image of the center of the tunnel to the ground surface. The reason for this behavior can be explained by the fact that the smaller the tunnel radius, the more the waves converge at the top of the tunnel. However, for a tunnel with a larger radius, the waves at the top of the tunnel diverge. By moving away from the tunnel, both models approach the free field. Therefore, the two curves are close to each other.

Figure 5(a) shows the effect of a change in tunnel radius on the ground spectral velocity for models 1 and 35 in

Table 1. Increasing the radius of the tunnel reduces the spectral velocity of the ground surface in the range of 0.84% to 12.3% depending on the distance of the study point from the tunnel. In Figure 5(b), the effect of change in the spectral velocity of the ground surface due to the increase of tunnel radius for models 10 and 14 of Table 1 is investigated. In Figure 5(b), (a) decrease in the spectral velocity of the ground surface is observed due to the increase in the radius of tunnel in the range of 0.36% to 7.63%, depending on the distance of the study point from the tunnel. Only at a point of 15.17 meters from the image of the center of the tunnel to the ground surface, a slight amount of spectral velocity is observed due to the increase of the tunnel radius by 0.38%.

In Figure 6(a), the effect of change in the spectral velocity of the ground surface due to the change of tunnel radius for

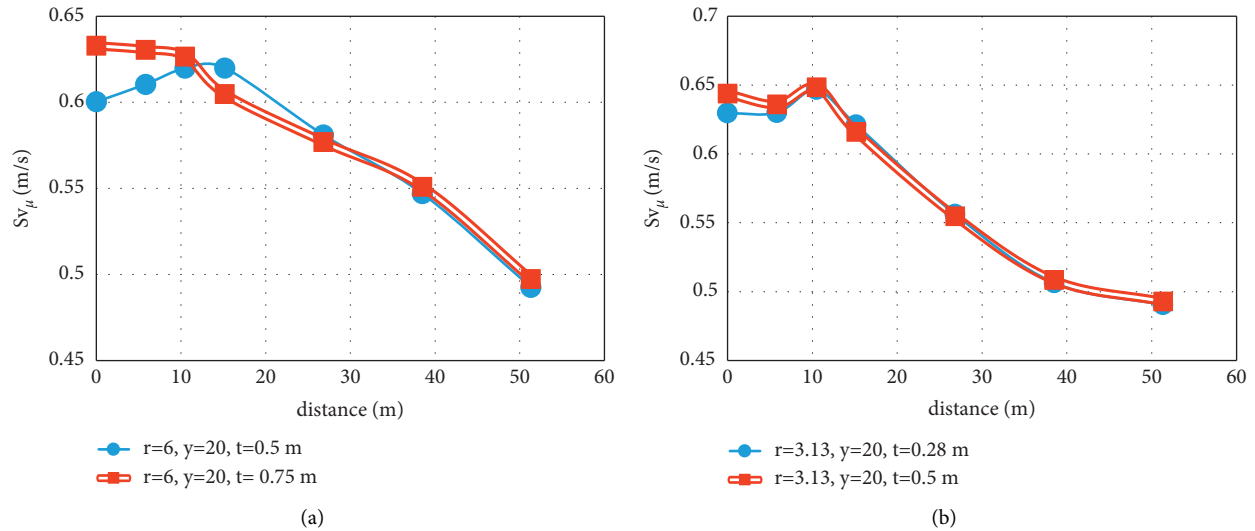


FIGURE 19: The effect of change in tunnel lining thickness on ground surface velocity for models (a) 24 and 25 and (b) 30 and 31 of Table 1.

models 20 and 24 in Table 1 is investigated. In Figure 6(a), increasing the tunnel radius has caused a decrease in the spectral velocity of the ground surface in the range of 0.23% to 7.84% depending on the distance of the study point from the tunnel. Figure 6(b) shows the effect of an increase in tunnel radius on the spectral velocity of the ground surface. Models 30 and 32 of Table 1 are examined in Figure 6(b). In Figure 6(b), a decrease in spectral velocity is observed due to the increase of the tunnel radius in the range of 0.79% to 7.81% depending on the distance of the study point from the tunnel. Only at a distance of 15.17 meters from the image of the center of the tunnel to the ground surface, 0.73% increase in spectral velocity due to the increase of the tunnel radius is observed.

The largest difference in the results of spectral velocity is related to the model of Figure 5(a), which is about 12.3% of the difference due to changes in radius, on the image of the center of the tunnel on the ground surface. That is, by increasing by about 92% of the tunnel radius, a maximum of 12.3% of the spectral velocity of the ground surface, depending on the model and intended point, is reduced.

In the next step, the effect of increasing the depth of the tunnel from 10 to 20 meters on the spectral velocity of the ground in different parts of the ground surface was investigated. The results are shown in Figures 7–14. Increasing the depth of the tunnel placement will have a different effect on the spectral velocity of the ground surface depending on the model. In most models (11 of the 15 models studied), increasing the depth of the tunnel placement will reduce the spectral velocity of the ground surface. In Figure 13(a), the maximum amount of spectral velocity reduction due to increasing the depth of the tunnel placement is equal to 4.42%. It occurs at a point with a distance of 5.83 meters (approximately equal to the tunnel radius) from the image of the tunnel center on the ground surface.

In 4 of the 15 models studied, increasing the depth of the tunnel placement increases the spectral velocity of the ground surface around the tunnel. The mentioned models

are shown in Figures 7(a), 8(a), 10(a), and 11(b). Figures 8(a), 10(a), and 11(b) include tunnels with a larger lining thickness (0.75 m) and a larger radius (6 m).

The highest amount of increasing in the spectral velocity of the ground surface which is due to the increase in the depth of the tunnel is related to Figure 8(a) and is equal to 12.13%. This value occurs at a distance of 5.83 meters (approximately equal to the radius of the tunnel) from the image of the center of the tunnel to the ground surface.

Also, the effect of change in the thickness of the tunnel lining on the spectral velocity of the ground surface in different places compared to the tunnel image was investigated. The results are shown in Figures 15–19. Changes in the thickness of the tunnel lining will have a different effect on the spectral velocity of the ground surface depending on the model. In tunnels with greater overhead depth (20 m), increasing the thickness of the tunnel lining increases the spectral velocity of the ground surface around the image of the center of the tunnel to the ground surface by a maximum of 10.86%, which is related to Figure 15(b). Also, in tunnels with greater overhead depth (20 meters), increasing the thickness of the tunnel lining causes a slight decrease in the spectral velocity of the ground surface, moving away from the image of the center of the tunnel. In tunnels with greater overhead depth (20 m), the largest difference in the spectral velocity of the ground surface due to the change in the thickness of the tunnel lining occurs exactly on the image of the tunnel center to the ground surface, and for tunnels with a larger radius (6 m), the amount of difference is greater. This trend is due to the fact that in models with larger tunnel radius, seismic waves hit with a larger obstacle. In other words, their divergence increases. As a result, the amount of the spectral velocity difference increases.

In tunnels with less overhead depth (10 m), increasing the thickness of the tunnel lining reduces the spectral velocity of the ground surface around the image of the center of the tunnel to the ground level by a maximum of 7.56% and is related to Figure 17(a). The greatest amount of decreasing in

the spectral velocity of the ground surface occurs due to the increase in the thickness of the tunnel lining for models with less overhead depth (10 m) approximately at a distance equal to the diameter of the tunnel from the image of the tunnel center to the ground surface.

The reason for the different effects of increasing the thickness of the lining on models with different placement depths can be explained as follows: the greater the depth of tunnel placement, the higher the thickness of the tunnel lining, the more rigid the seismic waves will hit a rigid obstacle and their irregularity will be more severe (it is thinner than the thickness of the tunnel lining). However, due to the large distance between the tunnel and the ground surface, the convergence of seismic waves at the top of the tunnel (thinner than the thickness of the tunnel lining) will be greater. Therefore, increasing the thickness of the tunnel lining in models with greater placement depth increases the spectral velocity around the tunnel on the ground surface. However, in models with shallower placement, as the thickness of the tunnel lining increases, seismic waves strike the barrier with greater rigidity. Therefore, the irregularity of seismic waves increases due to the increase in the thickness of the tunnel lining. However, due to the small distance of the tunnel from the ground surface, seismic waves cannot converge at the top of the tunnel. As a result, in tunnels with less placement depth, increasing the thickness of the tunnel lining reduces the spectral velocity of the ground surface around the tunnel.

In all Figures 5 to 19, the effect of changes in the behavior of the models is negligible by moving away from the image of the center of the tunnel, which indicates that the free field conditions and the dimensions of the models are correct.

4. Conclusions

- (1) A tunnel with a smaller radius will have a higher spectral velocity ($S_v\mu$) at the ground surface than a tunnel with a larger radius. By increasing the tunnel radius by about 92%, the maximum of the ground surface spectral velocity decreases by a maximum of 12.3%, depending on the model and intended point. By moving away from the image of the center of the tunnel on the ground surface, the difference between the values of spectral velocity for tunnels of different diameters will be less. The spectral velocity for a smaller diameter tunnel is generally reduced by moving away from the image of the center of the tunnel on the ground surface. The opposite is hold true for larger diameter tunnels.
- (2) In most of the studied models, the decrease in the spectral velocity of the ground surface will occur due to the increase of the tunnel depth from 10 to 20 meters. The maximum amount of spectral velocity reduction is due to the increase in tunnel placement depth is equal to 4.42% and occurs at points approximately equal to the tunnel radius. In a small number of studied models, an increase in the spectral velocity of the ground surface is observed due to the

increase in the depth of the tunnel. The maximum amount of increasing in the spectral velocity of the ground surface due to the increase in the depth of the tunnel placement is equal to 12.13% and occurs at a distance approximately equal to the radius of the tunnel from the image of the center of the tunnel to the ground surface.

- (3) In the present study, tunnels with two placement depths of low (10 meters) and high (20 meters) were investigated. In tunnels with greater overhead depth (20 meters), an increase in the spectral velocity of the ground surface around the image of the center of the tunnel to the ground surface by a maximum of 10.86% is observed due to the increase in the thickness of the tunnel lining. In the mentioned models, the biggest difference in the spectral velocity of the ground surface due to the change in the thickness of the tunnel lining occurs exactly on the image of the center of the tunnel to the ground surface and for tunnels with a larger radius (6 meters), the difference is greater. Increasing the thickness of the tunnel lining is caused to reduce the spectral velocity of the ground surface around the image of the center of the tunnel to the ground surface by a maximum of 7.56% for tunnels with a lower depth (10 meters). For models with less overhead depth (10 meters), at approximately equal distances from the tunnel diameter from the image of the center of the tunnel to the ground surface, the greatest amount of decrease in the spectral velocity of the ground due to increasing the thickness of the tunnel lining is observed. In all the studied models, by moving away from the image of the tunnel center, the effect of changing in the thickness of the tunnel lining on the spectral velocity of the ground surface decreases.

Data Availability

The data used to support the findings of this study are available from the corresponding author upon request.

Conflicts of Interest

The authors declare that they have no conflicts of interest.

References

- [1] N. M. Newmark, J. A. Blume, and K. K. Kapur, "Seismic design spectra for nuclear power plants," *Power Division ASCE*, vol. 99, no. PO2, pp. 287–303, 1973.
- [2] P. W. Basham, D. H. Weichert, F. M. Anglin, and M. J. Berry, "New probabilistic strong seismic ground motion maps of Canada," *Bulletin of the Seismological Society of America*, vol. 75, no. 2, pp. 563–595, 1985.
- [3] T. D. O'Rourke, H. E. Stewart, and S.-S. Jeon, "Geotechnical aspects of lifeline engineering," *Proceedings of the Institution of Civil Engineers - Geotechnical Engineering*, vol. 149, no. 1, pp. 13–26, 2001.

- [4] M. O'Rourke and G. Ayala, "Pipeline damage due to wave propagation," *J Geotech Eng ASCE*, vol. 119, no. 9, pp. 1490–1498, 1993.
- [5] M. E. Barenberg, "Correlation of pipeline damage with ground motions," *Journal of Geotechnical Engineering*, vol. 114, no. 6, pp. 706–711, 1988.
- [6] American Lifelines Alliance, "ALA.: Seismic Fragility Formulations for Water Systems. American Society of Civil Engineers (ASCE) and Federal Emergency Management Agency(FEMA)," 2001, <http://www.americanlifelinesalliance.org>.
- [7] O. Pineda and M. Ordaz, "Seismic vulnerability function for high-diameter buried pipelines: Mexico city's primary water system case," in *Proceedings of the 2003 ASCE International Conference on Pipeline Engineering and Construction*, July 2003.
- [8] S.-S. Jeon and T. D. O'Rourke, "Northridge earthquake effects on pipelines and residential buildings," *Bulletin of the Seismological Society of America*, vol. 95, no. 1, pp. 294–318, 2005.
- [9] Y. M. A. Hashash, J. J. Hook, B. Schmidt, J. I-Chiang Yao, and C. Yao, "Seismic design and analysis of underground structures," *Tunnelling and Underground Space Technology*, vol. 16, no. 4, pp. 247–293, 2001.
- [10] S. Toprak and F. Taskin, "Estimation of earthquake damage to buried pipelines caused by ground shaking," *Natural Hazards*, vol. 40, no. 1, pp. 1–24, 2007.
- [11] N. Makris and C. J. Black, "Evaluation of peak ground velocity as a "good" intensity measure for near-source ground motions," *Journal of Engineering Mechanics*, vol. 130, no. 9, pp. 1032–1044, 2004.
- [12] S. Akkar and Ö. Özen, "Effect of peak ground velocity on deformation demands for SDOF systems," *Earthquake Engineering & Structural Dynamics*, vol. 34, no. 13, pp. 1551–1571, 2005.
- [13] R. P. Orense, "Assessment of liquefaction potential based on peak ground motion parameters," *Soil Dynamics and Earthquake Engineering*, vol. 25, no. 3, pp. 225–240, 2005.
- [14] M. Bastami, "Seismic reliability of power supply system based on probabilistic approach," PhD Thesis, Kobe University, Kobe, Japan, 2007.
- [15] O. Pineda-Porras and M. Najafi, "Seismic damage estimation for buried pipelines: challenges after three decades of progress," *Journal of Pipeline Systems Engineering and Practice*, vol. 1, no. 1, pp. 19–24, 2010.
- [16] M.J. O'Rourke and X. Liu, "Seismic Design of Buried and Offshore Pipelines," *Monograph, MCEER-12-MN04*, MCEER, Buffalo, 2012.
- [17] I. Kongar, T. Rossetto, and S. Giovinazzi, "Seismic fragility of underground electrical cables in the 2010–11 Canterbury (NZ) earthquakes," in *Proceedings of the Second European Conference on Earthquake Engineering & Seismology*, Istanbul, Turkey, 2014.
- [18] M. Bastami and M. R. Soghrat, "Velocity spectrum for the Iranian plateau," *Journal of Seismology*, vol. 22, no. 1, pp. 83–103, 2017.
- [19] T. Saito, K. Morita, T. Kashima, and T. Hasegawa, "Performance of high-rise buildings during the 2011 great east Japan earthquake," in *Proceedings of the 15th World Conference of Earthquake Engineering*, Lisbon, Portugal, September 2012.
- [20] Architectural Institute of Japan, "Protecting high-rises against long period motions—wisdom to share among designers and engineers," vol. 2013, p. 513p, 2013 (in Japanese).
- [21] M. Gharizade Varnusfaderani, A. Golshani, and S. Majidian, "Analysis of cylindrical tunnels under combined primary near-fault seismic excitations and subsequent reverse fault rupture," *Acta Geodynamica et Geomaterialia*, vol. 14, no. No. 1, pp. 5–26, 2016.
- [22] H. Fakhriyeh, R. Vahdani, and M. Gerami, "Seismic acceleration spectrum of ground surface under urban subway tunnels with circular cross sections in soil deposits based on SSI," *Shock and Vibration*, vol. 2019, Article ID 2076961, 13 pages, 2019.
- [23] M. H. Baziar, M. R. Moghadam, K. Dong-Soo, and C. Y. Wook, "Effect of underground tunnel on the ground surface acceleration," *Tunnelling and Underground Space Technology*, vol. 44, pp. 10–22, 2014.
- [24] U. Cilingir and S. P. G. Madabhushi, "A model study on the effects of input motion on the seismic behaviour of tunnels," *Soil Dynamics and Earthquake Engineering*, vol. 31, no. 3, pp. 452–462, 2011.
- [25] M. Singh, M. N. Viladkar, and N. K. Samadhiya, "Seismic analysis of Delhi metro underground tunnels," *Indian Geotechnical Journal*, vol. 47, no. 1, pp. 67–83, 2016.
- [26] G. Chen, Q.-Y. Li, D.-Q. Li, Z.-Y. Wu, and Y. Liu, "Main frequency band of blast vibration signal based on wavelet packet transform," *Applied Mathematical Modelling*, vol. 74, pp. 569–585, 2019.
- [27] J. Lysmer and R. L. Kuhlemeyer, "Finite dynamic model for infinite media," *Journal of Engineering Mechanics Division*, vol. 95, pp. 859–878, 1969.
- [28] B. Sevim, "Nonlinear earthquake behaviour of highway tunnels," *Natural Hazards and Earth System Sciences*, vol. 11, no. 10, pp. 2755–2763, 2011.